Atom Indonesia

Journal homepage: https://atomindonesia.brin.go.id

Weighted CTDI Equation for 3D Rotational Angiography: A Monte Carlo Study

A. Azzi*, R. Hidayat, A. Rosa, L. E. Lubis

[1]*Departement of Physics, Faculty of Mathematics and Natural Sciences, Universitas Indonesia, Jl. Margonda Raya, Pondok Cina, Kecamatan Beji, Depok 16424, Indonesia*

ARTICLE INFO

Article history:
Received 17 February 2023
Received in revised form 23 December 2023
Accepted 6 January 2024

Keywords:

3D rotational angiography
CTDI
Monte Carlo
CBCT

ABSTRACT

This study aims to verify the weighted Computed Tomography Dose Index (CTDIw) coefficients of 3D rotational angiography (3DRA) procedure using Monte Carlo simulation. The Monte Carlo simulation EGSnrc usercode was employed for 3D dose simulations of the rotational angiography procedure. A virtual phantom resembles the head CTDI phantom was constructed, with a diameter of 16 cm and a density resembling polymethyl methacrylate (1.13 g/cm^3). A series of virtual phantoms consisting of 5 images with ionization chamber detectors at the center position, 12 o'clock, 9 o'clock, 6 o'clock, and 3 o'clock were acquired. Simulations were performed with photon sources of 70 and 109 kVp for 200-degree x-ray tube rotation. The field of view was divided into narrow, wide, and full beam with diameters of 1.7 cm; 4.9 cm; and 8.6 cm, respectively. The simulated doses at the ionization chamber were processed into weighting factor for weighted CTDI and compared with direct measurements. The dose ratio between peripheral and center positions for 360° CBCT and 200° 3DRA was 1:1 and 1:3 in this study. The weighting factors for 3DRA were determined as CTDIcenter = ¼ and CTDIperiphery = ¾. The measured average percentage difference of CTDIw between our weighted factor and conventional CTDIw was 1.75 % (-3.99 % to 6.08 %). The x-ray tube position of 3DRA impacted the accuracy of weighting factor of CTDIw, with implications for the proposed weighting factor (Wcenter = ¼ and Wperiphery = ¾) when using a 3DRA machine.

INTRODUCTION

Angiography is the gold standard of vascular imaging during interventional radiology, interventional cardiology, or invasive surgery. Recent advancements in rotational irradiation allows this modality to generate three-dimensional (3D) images known as 3D rotational angiography (3DRA). However, one of the main concerns in 3DRA is the medical radiation dose to patients. Mostly, the dose in angiography is assessed based on Dose Air Product (DAP) and effective doses [1]. Nonetheless, DAP based evaluation is not relevant to rotational procedure. The closest method to 3DRA is tomographic procedures like Computed Tomography (CT) scan. The fundamental dose descriptor for this procedure is the CT Dose Index ($CTDI_{100}$), which involves using a 100 mm long cylindrical ionization chamber and a cylindrical phantom for measurement. As a body representative, CTDI was measured at 5 points (1 central position and 4 peripheral positions), then weighted the results to obtain the average cross-sectional dose distribution called weighted CTDI ($CTDI_w$). The conventional $CTDI_w$ for a CT scan is defined by using Eq. (1).

$$CTDI_W = \frac{1}{3}(CTDI_{100})_{center} + \frac{2}{3}(CTDI_{100})_{periphery} \quad (1)$$

However, the values 1/3 and 2/3 serve as weighted coefficients to predict the average dose across all phantoms [2], and these coefficients are designed for fan beam computed tomography (FBCT) with full (360°) x-ray tube rotation.

The 3DRA irradiation employs cone beam computed tomography (CBCT) with a rotation of less than 360° [3]. These parameters have made conventional $CTDI_w$ unable to describe dose distribution in 3DRA. To accommodate CTDI measurements for CBCT, a previous study has advised using a point chamber in the middle of the beam [4] or pencil chamber with a length of 250 mm to cover all the secondary x-rays [5].

*Corresponding author.
E-mail address: akbar.azzi@sci.ui.ac.id
DOI: https://doi.org/10.55981/aij.2024.1307

However, most diagnostic radiology centers do not have access to point or 250 mm long pencil chambers to follow this recommendation. Consequently, the International Atomic Energy Agency (IAEA) published a protocol for using a 100 mm pencil chamber detector on a CBCT and a 32 cm diameter of the acrylic phantom. This protocol adds the ratio of the full beam width to the narrow plane beam width as close as 20 mm to the $CTDI_{100}$ formula [6]. Furthermore, there was a difference of $CTDI_w$ up to 10 % for a 200° and 18 % for a 180° rotation using the conventional equation [7,8].

In addition to measurements using detectors, several dose calculations regarding dose distribution in CT have also been developed, such as CT-Expo (G. Stamm, Hannover, and H.D. Nagel, Buchholz, Germany) [9] and Virtual Dose (NIBIB, USA) [10]. Evaluations of these software programs indicate that tube voltage parameters influence dose distribution, but other parameters such as beam collimation or radiation width do not significantly affect changes in CT dose distribution [11]. However, several studies have reported that another type of radiation width, as well as phantom geometries, impacts the weighted coefficients. Kim, Song et al. (2011) obtained the weighted coefficients with a ratio of 50:50 for the center and periphery of the phantom for > 40 mm irradiation width [12]. In addition, the Monte Carlo studies also proved that the weighted coefficients would change with the change of phantom geometries. The large range of diameter of the cylindrical phantoms reported that the weighting coefficient is more accurate with values of 3/8 and 5/8 for the center and periphery points than the conventional $CTDI_w$ [13]. As for the elliptical phantom, the weighting values vary linearly following the ratio of the major and minor phantom diameters [14]. In 2021, a Monte Carlo simulation method was also be used to predict weighted CTDI for CBCT and the optimum position of ion chamber measurement points [15].

This study aims to determine appropriate $CTDI_w$ weighted coefficient by utilizing the EGSnrc Monte Carlo code for a partial rotation on 3DRA C-arm machine and to compare the proposed coefficient with the conventional $CTDI_w$ equation.

METHODOLOGY

Monte Carlo of 3DRA

The Monte Carlo simulation modeled the delivered beam of 3DRA irradiation on the Siemens Artis Zee using two energy spectra i.e., 70 keV and 109 keV. The simulation was divided into two regions: x-ray tube (BEAMnrc) and CTDI head phantom (DOSXYZnrc). The components of the x-ray tube consisted of photon source and beam collimator. The x-ray source was defined using an x-ray spectrum generator based on a tungsten anode spectral model using interpolating polynomials (TASMIP) method with a tungsten target density of 8.96 g/cm^3 [16]. The spectrum results for each energy were then converted into *spectrum* format, which is readable for EGSnrc. In the source parameter, *source 1* (parallel rectangles of point sources) was chosen, with an energy limit for photons and electrons set at 10 keV, excluding the rest of the mass energy.

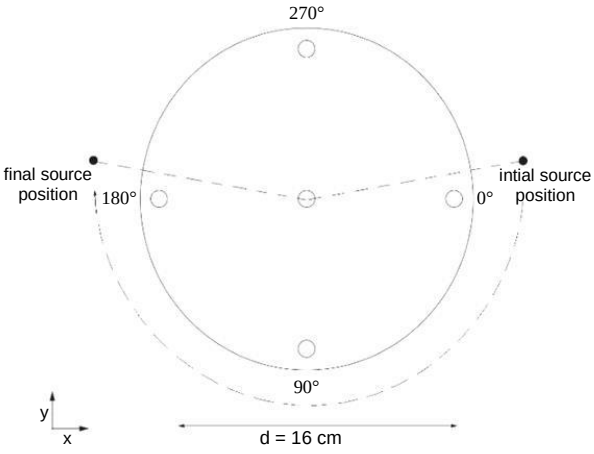

(a)

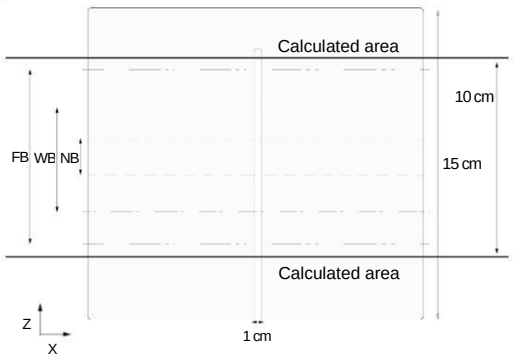

(b)

Fig 1. (a) Transversal plane of Virtual CTDI head phantom. A small circle inside the phantom showed an ion chamber positions of CTDI measurement. 0-degree position was at the 3 o'clock and X-ray tube rotated from 350° to 190° with clockwise direction (dash line). (b) Frontal plane view of CTDI phantom. Small cylinder at the center defined an example of air cavity as active volume. The algorithm calculated absorbed dose inside the air cavity within calculated area. NB, WB, and FB represented field width of narrow beam, wide beam, and full beam scan, respectively.

The lead collimator was used to shape the beam width. In this research, the CTDI phantom was irradiated with width of 1.7 cm, 4.9 cm, and 8.6 cm at the midpoint of the rotation. 1.7 cm was used to

accommodate for standard fan-beam CTDI measurement. The simulation results are stored in *.phps* format at the lower end of the collimator component. The second region was the Monte Carlo simulation in the CTDI head phantom using DOSXYZnrc usercode. The Siemens Artis Zee 3DRA machine's x-ray tube rotates by 200 degrees (from 80° to 280°), partially rotating under the phantom. For the source parameter, we selected *source 8* (phase space source from multiple direction) with multiangle irradiation features. The angle of simulation indicated the position of the x-ray tube at the time the radiation is delivered. Due to the difference in polar coordinate between the phantom geometry and DOSXYZnrc baseline, there was a 90° shift in the angular position. The initial position of phase space file was placed at 350° and ended at 190°. 500 million particle histories were used for each region, energy, and beam width in the Monte Carlo simulation. Figures 1a and 1b summarize the rotational position of the x-ray tube and the width of the irradiation beam in this study.

Five virtual phantoms were created for a diameter resembling CTDI head phantom following the design shown in Figure 1. The virtual phantom was constructed using MATLAB version 2021a (MathWorks, Natick, Massachusetts) with a homogeneous PMMA with a density of 1.13 g/cm^3 and voxel dimensions of 0.1 × 0.1 × 0.1 cm^3. The phantom had a diameter of 16 cm and a length of 15 cm. An air cavity with diameter of 1 cm and length of 13 cm was placed at each CTDI measurement point, as shown in the axial plane of the phantom (see Fig. 2). The design of the air cavity was aimed to ensure that the Monte Carlo simulation closely resembled the measurement situation inside an ion chamber, reducing systematic errors related to the mass-energy absorption ratio of medium and air. Subsequently, the virtual CTDI head phantom was converted into *.egsphant* format using *ct-create* user code.

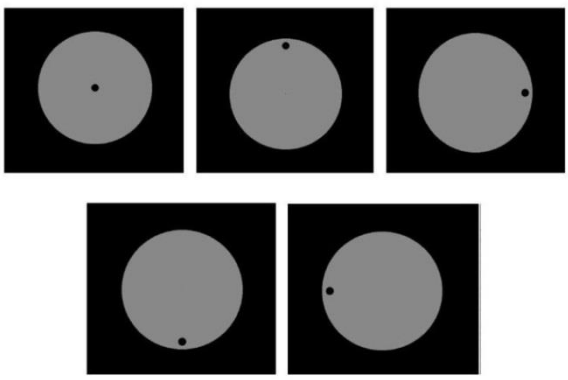

Fig 2. Transversal view of virtual phantom for center, 12, 3, 6, and 9 o'clock air cavity. Point doses were obtained by calculating energy deposition inside the cavity.

Relative dose calculation

The dose calculation in this simulation was conducted on the ion chamber's active volume. Numerically, the CTDI equation in this study can be expressed as follows in Eq. (2).

$$CTDI_{100} = \frac{1}{N}\sum_z \sum_r \sum_\theta D_p(rsin\theta, rcos\theta, z) \qquad (2)$$

where $CTDI_{100}$ and D_p represent CTDI in Monte Carlo simulation and dose point voxel inside the air cavity, respectively. N is the irradiation field width, including narrow, wide, and full beams. The simulated x-ray tube position (θ) ranges from 0.1 to 360 degree in discrete steps. The calculation position (r) represents the radius of air cavity and z was the calculation area in millimeters. Point position of $(r.sin\theta, r.cos\theta, z)$ corresponds to one voxel. Furthermore, the averaged dose cross section $\overline{D_{cs}}$ is given by Eq. (3).

$$\overline{D_{cs}} = \frac{1}{\pi R^2 NM}\sum_i \sum_z \sum_{r_{cs}} \sum_\theta D_p^i(r_{cs}sin\theta, r_{cs}cos\theta, z) \qquad (3)$$

Here, r_{cs} is the calculated position inside the phantom in axial plane, R is the phantom radius, D_p^i is the voxel dose at the specified position in every air cavity, and M is the total number of Monte Carlo simulation. The averaged dose $\overline{D_{cs}}$ in principle is equivalent to weighted CTDI.

CTDI measurement

Direct measurement on a 3DRA machine was conducted to verify the generated coefficients from the Monte Carlo simulation. CTDI measurements were performed using the IAEA protocol on Siemens Artis Zee 3DRA fluoroscopy. A Radcal 10X6-3CT ion chamber, which is 100 mm in length, was used and irradiated with two nominal tube voltage of 70 kV and 109 kV. In detail, the exposure factors in this study can be seen in Table 1.

Implementing the conventional weighted CTDI, $CTDI_{100}$ was partitioned into $CTDI_{center}$ and $CTDI_{periphery}$. The dose cross section is expressed as follows in Eq. (4).

$$\overline{D_{cs}} = w_1(CTDI_{100})_{center} + w_2(CTDI_{100})_{periphery} \qquad (4)$$

where w_1 and w_2 represent the $CTDI_w$ coefficients. The solution of this linear equation was obtained using MATLAB *linsolve* library, incorporating all energy and beam width parameters. Mathematically, the *linsolve* input can be written as follows.

$$\begin{pmatrix} (CTDI_{100})^{70\ kV,NB}{}_{center} & (CTDI_{100})^{70\ kV,NB}{}_{periphery} \\ \vdots & \vdots \\ (CTDI_{100})^{109\ kV,FB}{}_{center} & (CTDI_{100})^{109\ kV,FB}{}_{periphery} \end{pmatrix} \begin{pmatrix} w_1 \\ w_2 \end{pmatrix} = \begin{matrix} \overline{D_{cs}}^{70\ kV,NB} \\ \vdots \\ \overline{D_{cs}}^{109\ kV,FB} \end{matrix} \quad (5)$$

Table 1. Exposure factor of each measurement on 3DRA Artis Zee.

Parameter	20s DCT Head (70 kV)	20s DCT Head (109 kV)
Tube Voltage	70 kV	109 kV
Tube Current	236 mAs	169 mAs
Pulse Width	11.6 ms	7.3 ms
Time	20 s	20 s
Frame per second	3	3

Weighted CTDI coefficients and analysis

The proposed coefficient was analyzed by comparing the simulated CTDI with measured CTDI for the same exposure parameters, as well as with conventional $CTDI_w$ equation. By using the conventional $CTDI_w$ equation as a reference, the percentage difference in $CTDI_w$ was obtained as follows.

$$\Delta\% = \frac{\left(CTDI_W^{conv} - CTDI_W^{proposed}\right)}{CTDI_W^{conv}} \times 100\% \quad (6)$$

RESULTS AND DISCUSSION

500 million Monte Carlo particle histories yield an average standard deviation of 2.99 % in simulations, with a range of 1.83 % to 6.07 %. To validate the Monte Carlo method, a full rotation of the CBCT was simulated for all simulation parameters. Before applying Eq. (5), it is necessary to consider dependent factors, such as variations in beam width and energy. Based on the IAEA protocol regarding CBCT measurements using a 100 mm detector, a comparison of the $CTDI_{100}$ ratio between wide and narrow beams should be incorporated into the equation. In this study, the comparison between Full Beam (8.6 cm) and Narrow Beam (1.7 cm) yielded an average ratio of 0.965 ± 0.024 for 70 kV and 0.970 ± 0.023 for 109 kV. This ratio indicates that the conventional $CTDI_{100}$ equation can be used for measurements of CBCT with a 100 mm ion chamber without losing significant dose reading information. This result were supported by previous research conducted by Leon et al., which reported a 3 % difference between conventional CTDI collimated beam and open beam measurements [8]. Moreover, this explains that the energy variation used in this study did not substantially affect the dose-response. The Pearson correlations for the energy in function of field widths of the NB, WB, and FB beams showed strong correlations with r = 0.99, r = 0.87, and r = 0.98, respectively. These results are agreed with the research by Markovich et al., which stated that the variation in tube voltage (kV) is 2-5 % [14].

Figure 3a displays an axial view of normalized CTDI dose distribution with air cavity at the center of the phantom for one full rotation. The dose distribution was evenly distributed inside the phantom. Consequently, the weighting ratio of $CTDI_{center}$ and $CTDI_{pheriphery}$ in this study was 1:1. These results were consistent with the coefficient values obtained by Kim et al. for CBCT, where a ½ weighting factor was assigned to both the middle and periphery of the phantom [12]

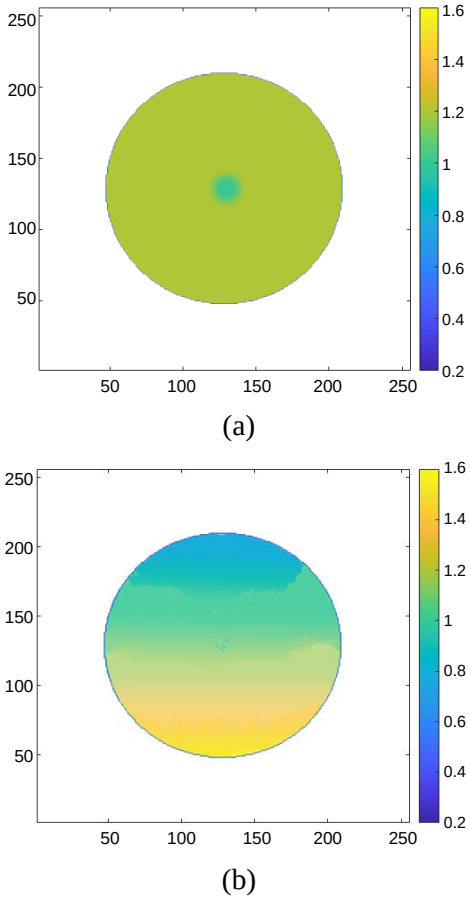

Fig 3. Typical dose distribution of CBCT Full Beam on Monte Carlo simulation with air cavity in the middle of the phantom for a) full and b) partial rotation. The partial rotation represents the 3DRA irradiation scanning of 200° rotating x-ray tube.

An example of the dose distribution in 3DRA irradiation is shown in Figure 3b. Visually, the dose is notably concentrated at the bottom of the phantom, attributed to the impact of the x-ray tube rotation during radiation. As weighted CTDI is a relative factor, the results of Monte Carlo simulations and measurements with an ionization chamber were normalized at the central position, as depicted in Table 2 and Fig. 4. There was a consistent trend between the simulation and ion chamber measurement, where the value at 12 o'clock being the lowest and 6 o'clock being the highest value. In general, Monte Carlo normalized CTDI values were smaller than the direct measurement. In contrast, at the 12 o'clock position, the simulated dose showed a higher value than the measurement. This discrepancy might be attributed to the absence of simulation for the patient table, which was a photon beam attenuator [17].

Table 2. Ratio of $CTDI_{position}/CTDI_{center}$ of Monte Carlo simulation and ion chamber measurement for each energy and position.

Energy (keV)	Position	Monte Carlo Simulation			Ion Chamber Measurement		
		NB	WB	FB	NB	WB	FB
70	$\overline{D_{cs}}$	0.89	0.91	0.88			
	Center	1	1	1	1	1	1
	12 o'clock	0.78	0.78	0.72	0.55	0.55	0.54
	3 o'clock	1.06	1.11	1.1	1.46	1.41	1.39
	6 o'clock	1.31	**1.4**	1.37	2.09	2.11	2
	9 o'clock	1.06	1.06	1.06	1.44	1.37	1.36
109	$\overline{D_{cs}}$	0.84	0.86	0.91			
	Center	1	1	1	1	1	1
	12 o'clock	0.77	0.74	0.77	0.55	0.56	0.55
	3 o'clock	0.98	1.04	1.11	1.42	1.58	1.56
	6 o'clock	1.19	1.2	1.31	2.05	2.22	2.19
	9 o'clock	0.97	1.01	1.11	1.4	1.53	1.52

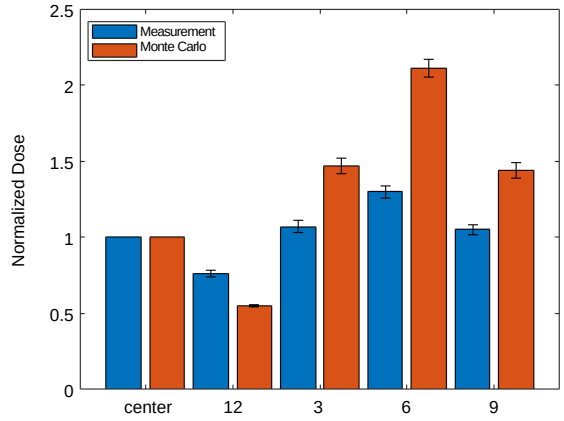

Fig 4. Average dose point at center, 12, 3, 6, and 9 o'clock ion chamber position for all energy and radiation width. The dose was normalized to center position of Head CTDI phantom.

Applying Eq. (5), the weighted CTDI coefficients derived in this study were found to be 0.26 for the center and 0.74 for the periphery. As a result, the proposed $CTDI_w$ equation for evaluation on the 3DRA machine is formulated as follows in Eq. (7).

$$CTDI_W = \frac{1}{4}(CTDI_{100})_{center} + \frac{3}{4}(CTDI_{100})_{periphery} \quad (7)$$

The $CTDI_w$ results for ion chamber measurements based on these proposed coefficients and the conventional equation are summarized in Table 3. Notably, the percentage differences between the proposed and conventional $CTDI_w$ were within -3 %. The negative sign signifies that the $CTDI_w$ dose obtained from the proposed equation was greater than the conventional method. This observed accuracy compares favorably with the average dose interpolation method, which reported a 6 % dose difference with the $CTDI_w$ conventional method for four ion chamber measurement positions on the CTDI phantom using the same machine [7].

Table 3. $CTDI_W$ different between conventional and proposed equation for 3DRA.

Energy (keV)	Field Width	$CTDI_W$ (mGy)		%Δ
		conventional	proposed	
70	NB	10.39	10.64	-2.41 %
	WB	9.81	10.10	-2.96 %
	FB	7.03	7.23	-2.84 %
109	NB	10.00	10.25	-2.50 %
	WB	10.47	10.73	-2.48 %
	FB	7.05	7.20	-2.13 %

There were limitations to this research. Firstly, simulations and measurements were conducted only on a 3DRA machine with a 200° rotation. As shown in Fig. 3, variation in the rotation during irradiation led to different dose distributions and coefficients of the $CTDI_w$. Investigating of the impact of the rotation angle of the x-ray tube on the weight coefficient is beyond the scope of this study. Secondly, this study focuses on theoretical Monte Carlo simulations and compares only with common ion chamber measurements. Further validation through experimental methods, such as using Gafchromic film could be undertaken to verify the average cross-section dose, which cannot be done using an ion chamber.

CONCLUSION

In this work, Monte Carlo simulation and linear solver techniques were performed to provide a more accurate average dose assessment for 3DRA

irradiation. The concept of weighted CTDI was successfully implemented on 3DRA by replacing the weighting coefficients with $W_{center} = 1/4$ and $W_{periphery} = 3/4$. The accuracy of proposed $CTDI_w$ equation differs by 3 % to conventional CTDI formula. These findings contribute valuable insights for estimating average doses using standard $CTDI_{100}$ protocol measurement on 3DRA.

ACKNOWLEDGMENT

This study was funded by Faculty of Mathematics and Natural Sciences Universitas Indonesia grant No. 019/UNF2.F3.D/PPM.00.002/2022

AUTHOR CONTRIBUTION

All authors read and approved the final version of the paper.

REFERENCES

1. X. Li, J. A. Hirsch, M. M. Rehani *et al.*, Am. J. Roentgenol. **214** (2020) 158.
2. W. Leitz, B. Axelsson and G. Szendrö, Radiat. Prot. Dosim. **57** (1995) 377.
3. T. Berris, R. Gupta and M. M. Rehani, Am. J. Roentgenol. **200** (2013) 755.
4. R. Fahrig, R. Dixon, T. Payne *et al.*, Med. Phys. **33** (2006) 4541.
5. Y. Kyriakou, P. Deak, O. Langner *et al.*, Phys. Med. Biol. **53** (2008) 3551.
6. International Atomic Energy Agency (IAEA), IAEA Human Health Series Report 5, Status of Computed Tomography Dosimetry for Wide Cone Beam Scanners, Vienna (2011).
7. E. C. Podnieks and I. S. Negus, Br. J. Radiol. **85** (2012) 161.
8. S. Leon, J. Appl. Clin. Med. Phys. **18** (2017) 230.
9. U. Lechel, C. Becker, G. Langenfeld-Jäger *et al.*, Eur. Radio. **19** (2009) 1027.
10. A. Ding, Y. Gao, H. Liu *et al.*, Phys. Med. Biol. **60** (2015).
11. C. De Mattia, F. Campanaro, F. Rottoli *et al.*, Eur. Radiol. Exp. **4** (2020) 1.
12. S. Kim, H. Song, E. Samei *et al.*, J. Appl. Clin. Med. Phys. **12** (2011) 84.
13. T. Haba, S. Koyama, Y. Kinomura *et al.*, Med. Phys. **44** (2017) 6603.
14. A. Markovich, A. G. Morgan, F. F. Dong *et al.*, J. Med. Imaging **4** (2017) 031205.
15. T. Haba, K. Yasui, Y. Saito *et al.*, Physica Med. **81** (2021) 130.
16. J. M. Boone and J. A. Seibert, Med. Phys. **24** (1997).
17. A. Abuhaimed, C. J. Martin, M. Sankaralingam, *et al*., Phys. Med. Biol. **60** (2015) 1519.